

Supplemental Information

Dual model biosensor integrated with peroxidase-like activity and self-assembly for uric acid detection

Dingyitai Liang[#], Ziqi Ding[#], Yushu Ding, Wenxuan Tang, Shouzhi Yang, Xiaoyu Xu, Yuning Wang, Kun Qian**

State Key Laboratory of Systems Medicine for Cancer, School of Biomedical Engineering and Institute of Medical Robotics, Shanghai Jiao Tong University, Shanghai 200030, P. R. China

[#]These authors contributed equally to this work.

Email: yuningwang@sjtu.edu.cn; k.qian@sjtu.edu.cn

Experimental procedures

1. Chemical reagents and apparatus

Chloroauric acid ($\text{HAuCl}_4 \cdot 4\text{H}_2\text{O}$, 47.8%), acetic acid (99%), ethanol (99.7%), and hydrogen peroxide (30%) were obtained from Sinopharm. Copper chloride (CuCl_2 , 99.9%), NaOH (95%), uricase (20 U/mg), and L-Ascorbic acid (AA, 99%) were obtained from Macklin. Dimethyl sulfoxide (DMSO, 99.8%), dichloroethane (DCE, 99.8%), dopamine (99%), sodium acetate (99%), and guanine (99%) were obtained from Aladdin. 3,3',5,5'-tetramethylbenzidine (TMB, 99%), L-glutamic acid (99.5%), L-lysine (98%), D-glucose (99.5%), and L-aspartic acid (98%) were obtained from Sigma-Aldrich. Heptadecafluorooctanesulfonic acid potassium salt (PFOSK, 98%) was obtained from J&K Scientific. Uric acid (99%) was obtained from Ourchem. The CheKine™ Uric Acid (UA) Colorimetric Assay Kit purchased from Abbkine. All deionized (DI) water used in this study was obtained by Milli-Q Advantage A10.

The image of scanning electron microscopy (SEM) was collected by Hitachi S-4800. The images of transmission electron microscopy (TEM), high resolution TEM, elemental mapping, and selected-area electron diffraction pattern were obtained by JEOL JEM-2100F. The experiment of ultraviolet-visible (UV-vis) absorption was performed on UV 1900 spectrophotometer. The surface roughness (Sa) of the co-crystallization of materials and biosamples was measured by a 3D laser scanning microscope VK-X3000. All the laser desorption/ionization mass spectrometry (LDI-MS) analysis was performed by Bruker Autoflex III MALDI TOF/TOF mass spectrometer.

2. Synthesis of the h-Cu₂O NCs and Cu₂O@Au NCs

The hollow Cu₂O NCs were prepared by adding CuCl₂ micro-powder into aqueous HCl (pH=0.5) and reacted with DI water at pH 6.5 for 0.5 h at room temperature (RT)¹. As shown in Fig. S2, the SEM and TEM images of the product illustrated the inside hollow structure of Cu₂O NPs.

In order to synthesize the Cu₂O@Au NCs, 15 mg of the Cu₂O were first dissolved in 10 mL of DI water by ultrasonic dispersion for 10 min. Then, 40 mg of sodium citrate

was added with stirring at RT. After stirring for 15 min, 0.5 mL of HAuCl_4 (5 mM) was added dropwise into with the color of the mixture turning into brown black immediately, which implies the generation of AuNPs. After stirring for another 20 min, the $\text{Cu}_2\text{O}@Au$ NCs were collected by centrifugation and washed several times. As shown in the SEM, TEM and element mapping images in Fig. S3, the AuNPs are uniformly distributed on the surface of the Cu_2O NCs, demonstrating the successful synthesis of the $\text{Cu}_2\text{O}@Au$ NCs.

3. UA adsorption behavior under varying pH and ionic strength conditions

For the pH-dependent adsorption experiment, the UA solution (2 mM, 100 μL) with different pH values of 3, 5, 7, or 9 was mixed with h- $\text{Cu}_2\text{O}@Au$ (1.2 mg/mL, 100 μL) and incubated at RT for 30 min. As control, the original condition was UA in DI water (1 mM, 200 μL). For the ionic strength-dependent adsorption experiment, UA (3 mM in PBS, 100 μL) was mixed with h- $\text{Cu}_2\text{O}@Au$ (1.2 mg/mL, 100 μL) and NaCl solution (100 μL) at varying concentrations (0, 10, 50, 100, 500 mM), followed by incubation at RT for 30 min. As control, the original condition was UA in DI water (1mM, 300 μL). After incubation, we obtained the supernatant by centrifugation at 10,000 rpm for 10 min, and calculated the concentration of UA in the supernatant by the colorimetry method.

4. Harvest of clinical serum and urine samples

All serum and urine samples from human participants were provided by Shanghai Renji Hospital (Shanghai, China), including 13 serum samples and 13 urine samples, and all works in this research were approved by the ethics committee of Shanghai Renji Hospital (Shanghai, China, IRBKY2022-001-B). As for serum sample collection, the blood samples underwent centrifugation at 5000 r/min for 10 min at 4 °C to obtain the serum supernatant, which was promptly stored at -80°C for later use. As for urine sample collection, 5 mL of collected urine per individual was centrifuged at 3000 r/min for 10 min at 4 °C and the resulting supernatant urine samples were also stored at -80 °C until needed. Subsequently, serum and urine samples were diluted 5 times and 40 times respectively, storing at -80°C for further use.

Safety statement

No unexpected or unusually high safety hazards were encountered in this work.

Supplementary figures

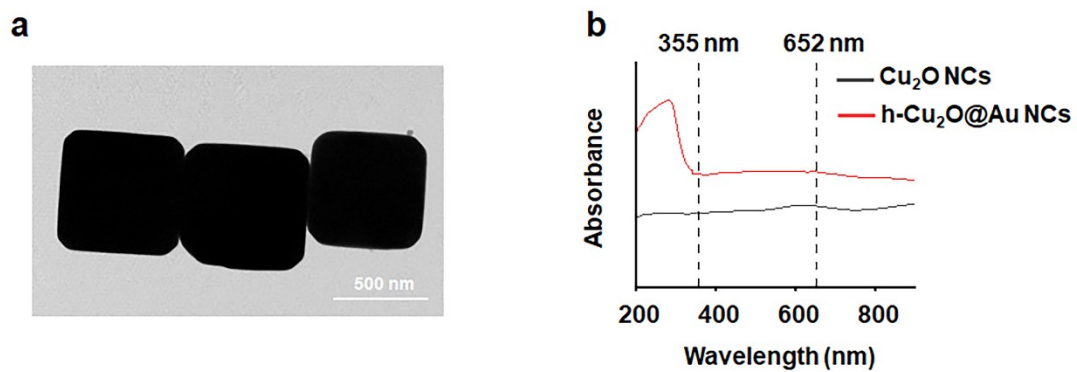


Fig. S1. (a) Low-magnification TEM image of Cu_2O NCs. (b) The UV-vis absorption spectra of Cu_2O NCs (black) and $\text{h-Cu}_2\text{O@Au}$ NCs (red).

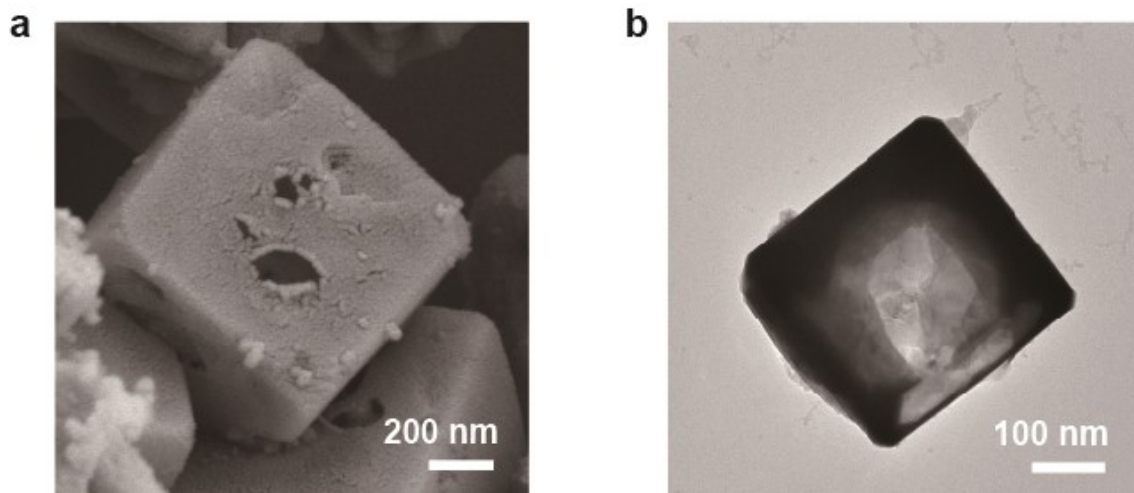


Fig. S2. The characterization of h-Cu₂O NCs. (a) The SEM image of h-Cu₂O NCs. (b) The TEM image of the h-Cu₂O NCs. The scale bars are 200 nm (a) and 100 nm (b), respectively.

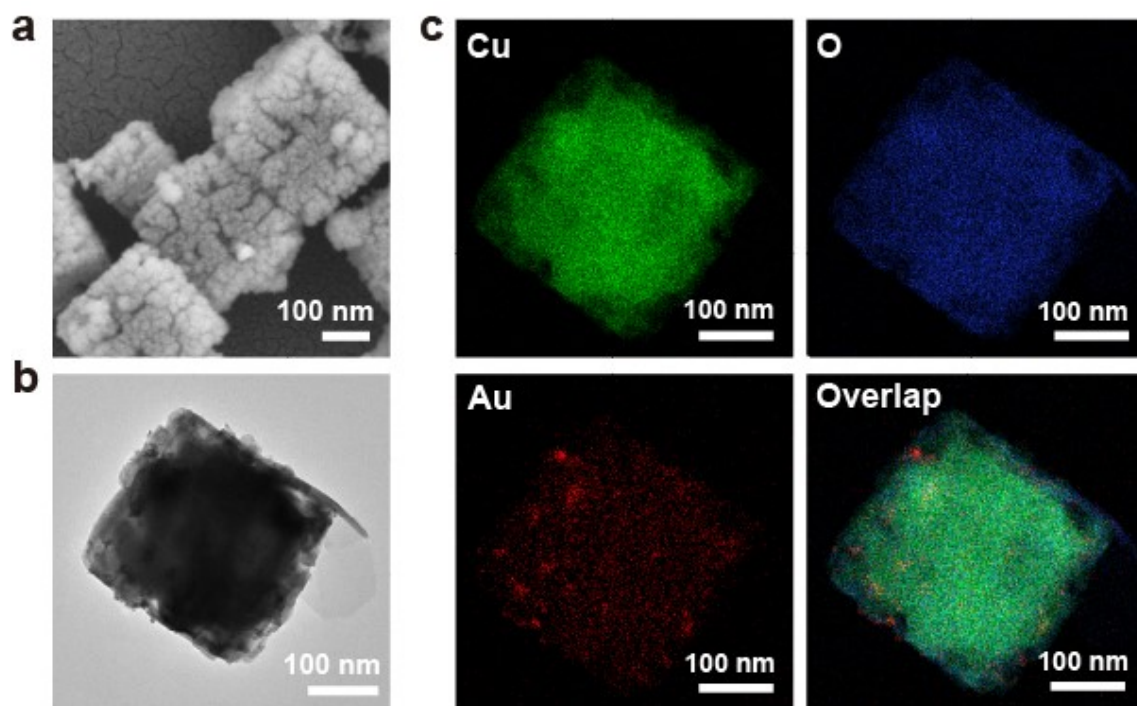


Fig. S3. The characterization of Cu₂O@Au NCs. (a) The SEM image of the Cu₂O@Au NCs. (b) The TEM image of Cu₂O@Au NCs. (c) The element mapping images of Cu₂O@Au NCs, containing Cu (green), O (blue), and Au (red). The scale bars are 100 nm.

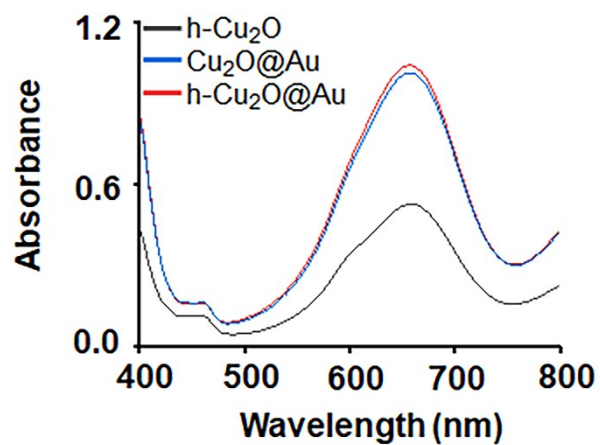


Fig. S4. The POD-like activity of h-Cu₂O@Au NCs as nanozyme. The UV-vis absorbance spectra of different systems, including h-Cu₂O@Au NCs+TMB+H₂O₂ (red curve), Cu₂O@Au NPs+TMB+H₂O₂ (blue curve), and h-Cu₂O+TMB+H₂O₂ (black curve).

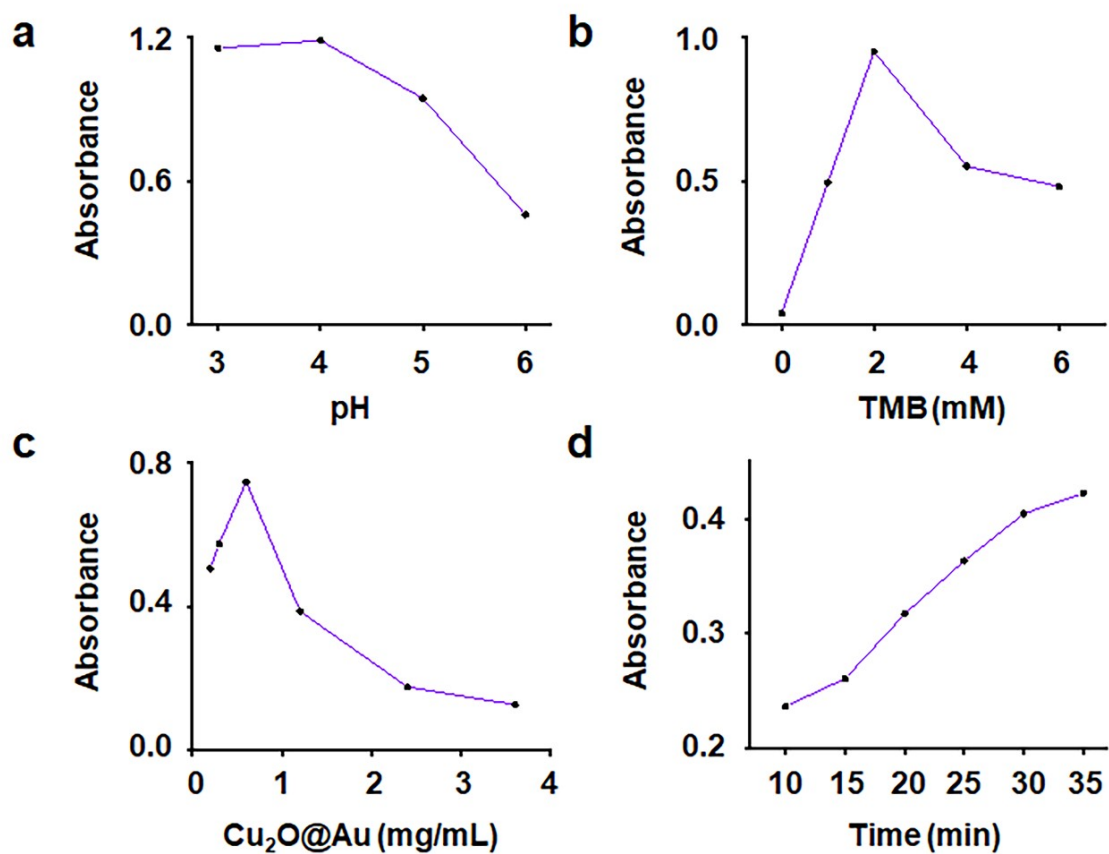


Fig. S5. The optimization conditions for POD-like activity of h-Cu₂O@Au NCs, including (a) pH, (b) TMB concentration, (c) h-Cu₂O@Au NCs concentration, and (d) incubation time. Each error bar represents the standard deviation calculated from three replicates.

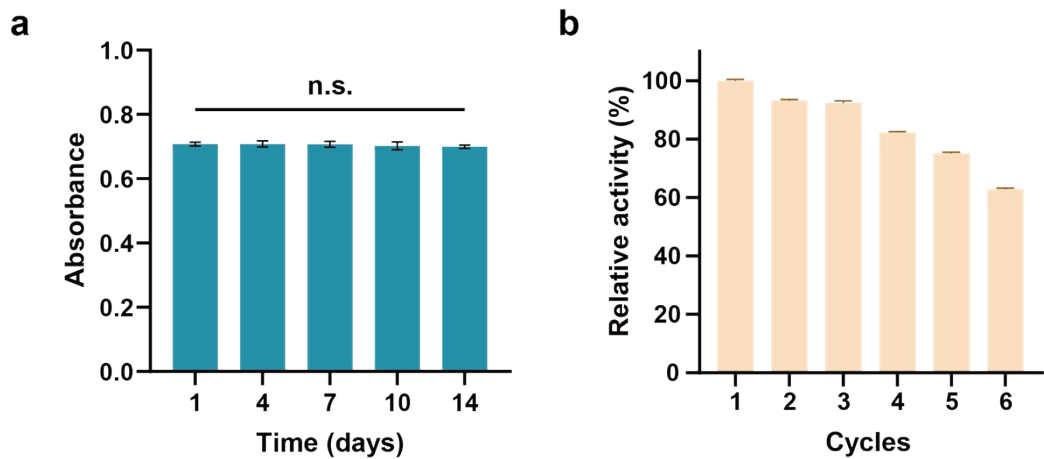


Fig. S6. Reproducibility and reusability test of h-Cu₂O@Au NCs. (a) Long-term stability of h-Cu₂O@Au NCs as nanozyme. The percentage was obtained based on the maximum absorbance recorded at 652 nm (p values: n.s., $p > 0.05$). (b) The reusability of h-Cu₂O@Au NCs as nanozyme for UA detection by colorimetry assay. Each error bar represents the standard deviation calculated from three replicates.

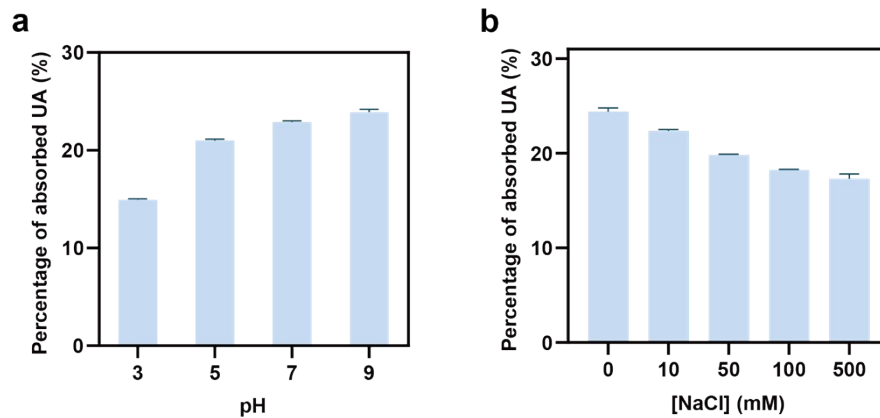


Fig. S7. UA adsorption efficiency under different (a) pH and (b) NaCl concentrations.

Error bars represent the standard deviation from three replicates.

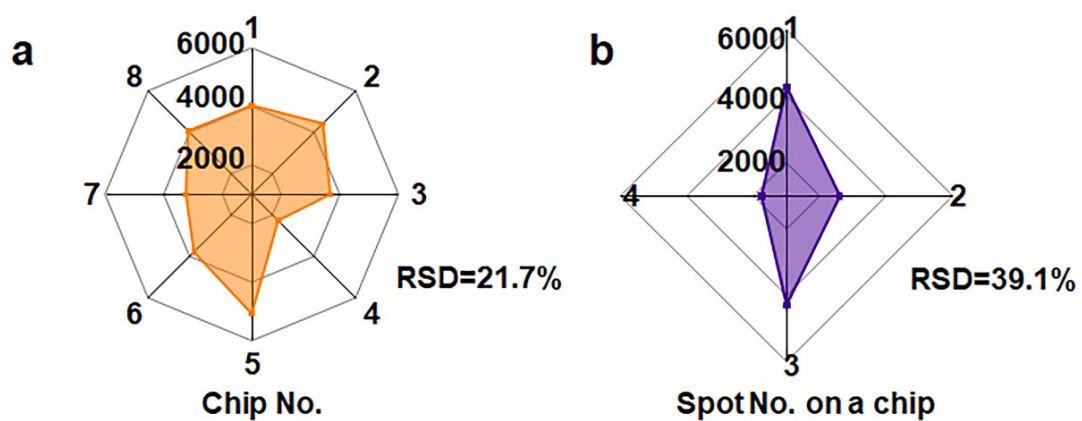


Fig. S8. The MS signal reproducibility of non-assembled h-Cu₂O@Au NCs as matrix for LDI-MS analysis of UA from (a) eight chips at random positions, and (b) four different spots on one chip.

Table S1. The comparison of kinetic parameters of h-Cu₂O@Au NCs with other catalysts.

Catalyst	Substrate	K_m (mM)	V_{max} (M·s ⁻¹)
h-Cu ₂ O@Au NCs (this work)	H ₂ O ₂	336.57	39.10×10 ⁻⁸
	TMB	5.23	18.08×10 ⁻⁸
Fe ₃ O ₄ MNPs ²	H ₂ O ₂	154	9.78×10 ⁻⁸
	TMB	0.098	3.44×10 ⁻⁸
HRP ²	H ₂ O ₂	3.70	8.71×10 ⁻⁸
	TMB	0.434	10.00×10 ⁻⁸
TA@AuNFs ³	H ₂ O ₂	37.34	129.87×10 ⁻⁸
	TMB	3.01	25.64×10 ⁻⁵
Au@Cu ₂ O ⁴	H ₂ O ₂	29.30	11.67×10 ⁻⁸
	TMB	0.202	27.22×10 ⁻⁸
Pb-FNA-Ag@Pt ⁵	H ₂ O ₂	216.2	44.4×10 ⁻⁶
	TMB	1.7	20.9×10 ⁻⁶

Reference

1. H. Liu, Y. Zhou, S. A. Kulinich, J.-J. Li, L.-L. Han, S.-Z. Qiao and X.-W. Du, *Journal of Materials Chemistry A*, 2013, **1**, 302-307.
2. L. Gao, J. Zhuang, L. Nie, J. Zhang, Y. Zhang, N. Gu, T. Wang, J. Feng, D. Yang and S. Perrett, *Nature Nanotechnology*, 2007, **2**, 577-583.
3. D. Liang, S. Yang, Z. Ding, X. Xu, W. Tang, Y. Wang and K. Qian, *ACS Nano*, 2024, **18**, 23625-23636.
4. J. Zeng, C. Ding, L. Chen, B. Yang, M. Li, X. Wang, F. Su, C. Liu and Y. Huang, *ACS Applied Materials & Interfaces*, 2023, **15**, 378-390.
5. Z. Du, L. Zhu, P. Wang, X. Lan, S. Lin and W. Xu, *Small*, 2023, **19**, 2301048.